

Diversity-Assisted Channel Estimation and Multiuser Detection for Downlink CDMA With Long Spreading Codes

Zhengyuan Xu, *Senior Member, IEEE*, Ping Liu, *Student Member, IEEE*, and Michael D. Zoltowski, *Fellow, IEEE*

Abstract—In downlink communication of a direct-sequence (DS) code-division multiple-access (CDMA) system, each user's short spreading codes are superimposed by base station's common long codes. This situation creates much difficulty in blind signal detection when multipath propagation occurs. However, when spatial/temporal diversity is available at the receiver, it is shown in this paper that subspace technique can be directly applied to estimate the common downlink multipath channel. Then, typical linear receivers, such as zero-forcing (ZF), minimum mean-square-error (MMSE) and RAKE receivers can be designed to detect the desired signal. Since the data covariance matrix is used but estimated from finite data samples, performance of both channel estimator and receivers gets perturbed. It is thus thoroughly and jointly analyzed by perturbation analysis. Justification of analysis and comparison of different receivers are also made through simulations.

Index Terms—Downlink, long codes, receiver diversity.

I. INTRODUCTION

DIRECT-SEQUENCE (DS) code division multiple access (CDMA) spread spectrum technology has been adopted in the new communication standards [1], [2]. It provides a communication system unique capabilities of simultaneous spectrum sharing, mitigation of jamming, interception, and multipath fading [3].

Despite those advantages, a DS/CDMA system is interference limited mainly due to multiuser interference (MUI). Significant efforts have focused on developing multiuser detection techniques for interference suppression [4]. In a DS/CDMA framework, either bit-level time-invariant codes (short codes) or pseudo-random codes (long codes) can be employed to spread the signal bandwidth. In a short-code CDMA system, spreading codes repeat from bit to bit, while in a long-code CDMA system, they vary with time. Most contributions assume short code spreading, resulting in simplified methods, adaptability to a changing environment, and, very importantly, tractable analysis

of the system performance. However, the spreading sequence to be adopted for the new-generation wireless systems is aperiodic with period much longer than the bit duration [1], [2]. Employment of long codes can increase immunity of the system to MUI and channel fading on the average [5]. Spreading by pseudo-random codes can also uniformly distribute the signal bandwidth, thus improving the spectrum efficiency. Moreover, they ensure a secure communication link in a hostile environment, protecting users' information against intentional interception.

However, previously mentioned advantages are achieved at the expense of increased complexity of the system structure. Long spreading codes inevitably destroy cyclostationarity of CDMA signals, making many of the existing channel estimation and detection approaches for short-code CDMA systems not directly applicable. Therefore, solutions for long-code CDMA systems are still under extensive investigation. Since Klein *et al.* applied a channel equalization idea to CDMA uplink [6], various ways to detect signals have been studied by employing a space-time two-dimensional (2-D) RAKE receiver structure and maximizing the signal-to-interference-plus-noise ratio (SINR) [7], [8] or by space-frequency processing [9]–[11]. An iterative maximum likelihood (ML) multiuser channel estimator is formulated in [12]. Using the finite alphabet property of the input, an iterative least-square method to estimate channel and inputs is developed [13]. Given pilot symbols of all users, iterative ML approaches are presented [5], [14]. Built upon the structure of convolutive channels, a Toeplitz displacement channel method has appeared [15]. Correlation matching techniques have been successfully applied for channel estimation [16]. Low complexity in channel estimation algorithms can be achieved when statistics of the spreading codes are given or estimated on-line [17]. A computationally efficient minimum mean-square-error (MMSE) detection approach is proposed in [18]. A novel parallel factor analysis technique is applied to multiuser detection [19]. Even in the presence of colored Gaussian noise in addition to unknown multipath fading and MUI, turbo multiuser detectors can be developed [20]. Performance of long-code CDMA systems and detection methods has also been extensively studied, from spectral efficiency [21], [22] to near-far resistance of MMSE detection [23] and tradeoffs of long versus short spreading sequences [24], [25]. Performance of ML detectors is studied [26] for multirate CDMA systems.

Due to currently extreme asymmetry, more research has been conducted for CDMA downlink than uplink. In downlink, user-specific short Hadamard codes are combined with the base

Manuscript received December 15, 2002; revised March 31, 2003. Z. Xu and P. Liu were supported by the U.S. National Science Foundation under Grant NSF-CCR 0207931. M. Zoltowski was supported by the U.S. Air Force Office of Scientific Research under Contract F49620-97-1-0275. The associate editor coordinating the review of this paper and approving it for publication was Prof. Brian Hughes.

Z. Xu and P. Liu are with the Department of Electrical Engineering, University of California, Riverside, CA 92521 USA (e-mail: dxu@ee.ucr.edu, pliu@ee.ucr.edu).

M. D. Zoltowski is with the School of Electrical Engineering, Purdue University, West Lafayette, IN 47907-1285 USA (e-mail: mikedz@ecn.purdue.edu).

Digital Object Identifier 10.1109/TSP.2003.820087

station's long codes to spread the signal spectrum. Although codes' orthogonality is destroyed by multipath propagation, it can be restored at the receiver by channel equalization [27]. Then, the user's information sequence is detected by despreading based on orthogonality of different codes. By forcing its output to be orthogonal to the subspace spanned by an unused code set, a blind equalizer is derived [28]. Assuming perfect channel information, comparisons are made among downlink symbol-level and chip-level zero-forcing (ZF), MMSE, and RAKE receivers in both single- and multiple-cell environments [29]–[31]. If two downlink channels are available in a mobile handset, a cross-correlation method [32] is successfully applied for channel estimation [33]. For sparse downlink multipath channels, reduced-rank MMSE equalization is shown to be very effective in multiuser detection [34], [35]. A generalized RAKE receiver structure and its optimization procedure are independently introduced in [36] and [37]. Downlink channel equalization is also contributed by [38]–[40]. Blind maximum SINR receivers can be directly derived [41], [42]. Based on a subspace concept, blind or pilot symbol-assisted subspace channel estimation methods are proposed in [43], assuming codes of a group of users are given. If all spreading codes are assumed random and unknown, a subspace technique has been applied to estimate multipath parameters in [44]. Semi-blind channel estimation solutions via subspace-based data projection are derived [45].

In this paper, we propose a diversity-aided downlink channel estimation method for a single-cell system where only intra-cell interference is of our interest. Then, we construct different linear equalizers/receivers using the estimated channel parameters. Since direct blind equalization is imperfect in the absence of diversity in downlink, we employ spatial/temporal diversity for both channel estimation and equalization purposes. Through diversity, signal subspace and noise subspace are created and separated in the received signal space. Thus, one of the most efficient techniques (the subspace technique) can be applied to estimate common downlink channels. Then different linear receivers are designed as in [30] and [31], i.e., using orthogonality of codes from different users to despread the output of the channel equalizer and extract the desired signal. However, the channel estimator is perturbed when the data covariance is estimated from finite number of received data samples. Meanwhile, performance of linear detectors largely depends on the designed channel estimator. Under a large sample size assumption, we apply the perturbation technique to jointly analyze the channel estimator and those detectors. Results on the second-order statistics of the sample covariance [46] turn out to be extremely helpful to achieve our goal. Simulation study shows high consistency between our analyses and numerical results.

This paper is organized as follows. A long-code CDMA downlink system model is described in Section II. A subspace-based channel estimation method is proposed in Section III, and implementation of three linear detectors is presented Section IV. Performance of channel estimator and receivers in terms of channel mean-square-error (MSE), receivers' SINR, and bit-error-rate (BER) are discussed in Section V. Finally, various simulation examples are provided in Section VI, and conclusions are drawn in Section VII.

II. CDMA DOWNLINK WITH LONG CODES

Consider a base station communicating with J mobile stations in a CDMA system. The j th user's aperiodic spreading codes at time n $c_{j,n}(k)$ ($k = 0, \dots, P-1$), which are the combination of its Hadamard codes and base station's long codes, are used to spread bit $w_j(n)$. Let the chip sequence be transmitted through M subchannels with unknown coefficients $g_m(k)$ for the m th subchannel. Such subchannels can be created by either oversampling the received data at a rate higher than chip rate or employing multiple receiver antennas. Each subchannel is assumed to be FIR and has order q ($q < P$). Then, the chip-level discrete-time signal due to the m th subchannel is a superposition of signals from J users corrupted by noise [44]

$$y_m(k) = \sum_{j=1}^J \sum_{l=0}^q g_m(l) s_j(k-l) + v_m(k) \quad (1)$$

$$s_j(k) = \sum_{n=-\infty}^{\infty} w_j(n) c_{j,n}(k-nP) \quad (2)$$

where $v_m(n)$ is the white Gaussian noise with variance σ_v^2 . Collecting P chip rate samples $[y_m(nP), \dots, y_m(nP+P-1)]$ from each subchannel and arranging samples from all M subchannels in a big vector yields

$$\mathbf{y}_{nP} = [y_1(nP), \dots, y_m(nP), \dots, y_1(nP+P-1), \dots, y_m(nP+P-1)]^T. \quad (3)$$

Using (1) through (3), a vector form data model follows:

$$\mathbf{y}_{nP} = \mathcal{G} \mathbf{b}_{nP} + \mathbf{v}_{nP}, \quad \mathbf{b}_{nP} = \sum_{j=1}^J \mathbf{b}_{j,nP} \quad (4)$$

where \mathcal{G} is a $MP \times (P+q)$ block Toeplitz matrix with P sub-blocks. The first block row of \mathcal{G} is $[\mathbf{G}, \mathbf{0}]$, and the $(i+1)$ th block row is obtained by right shifting the i th block row by one column. The kernel matrix \mathbf{G} is given by

$$\mathbf{G} = \begin{bmatrix} g_1(q) & \cdots & g_1(0) \\ \vdots & & \vdots \\ g_M(q) & \cdots & g_M(0) \end{bmatrix}. \quad (5)$$

In addition, in (4), \mathbf{b}_{nP} is a sum signal from all users. The j th user's combined input $\mathbf{b}_{j,nP}$ includes its transmitted bits and codes in the following way:

$$\mathbf{b}_{j,nP} = [w_j(n-1) \bar{\mathbf{c}}_{j,n-1}^T, w_j(n) \mathbf{c}_{j,n}^T]^T \quad (6)$$

where

$$\begin{aligned} \mathbf{c}_{j,n} &= [c_{j,n}(0), \dots, c_{j,n}(P-1)]^T, \\ \bar{\mathbf{c}}_{j,n-1} &= \mathbf{c}_{j,n-1}(P-q : P-1). \end{aligned} \quad (7)$$

\mathbf{b}_{nP} can be treated as a combined input from all users with $P+q$ elements. If $M > 1$, (4) virtually represents a single input multiple output (SIMO) system [47]. In this case, \mathcal{G} becomes a tall matrix. Then, the column space is invariant and well defined. Thus, the subspace method is readily applicable to estimate all subchannels. However, it can be easily observed that if we focus on the signature waveform of the transmitted bit

that is the channel convolved with long spreading codes, then the subspace spanned by signature waveforms varies from bit to bit, rendering the subspace method not directly applicable.

III. SUBSPACE-BASED DOWNLINK CHANNEL ESTIMATION

From our previous analysis, all columns of \mathcal{G} span the subspace of combined input \mathbf{b}_{nP} , which is time invariant. For convenience, this subspace is termed as signal subspace in this paper. Define columns of \mathcal{G} as h_i for $i = -q, \dots, 0, \dots, P-1$, and collect all unknown channel parameters in an $M(q+1) \times 1$ vector

$$\mathbf{h} = [g_1(0), \dots, g_M(0), g_1(1), \dots, g_M(1), \dots, g_1(q), \dots, g_M(q)]^T. \quad (8)$$

Then, $h_0 = [\mathbf{h}^T, 0, \dots, 0]^T$ with $MP - M(q+1)$ zeros. If we define an $MP \times M(q+1)$ matrix

$$\mathbf{A} = \begin{bmatrix} \mathbf{I}_{M(q+1)} \\ \mathbf{0} \end{bmatrix} \quad (9)$$

where \mathbf{I} is an identity matrix, then $h_0 = \mathbf{A}\mathbf{h}$. Other columns h_i also contain partial/full copies of vector \mathbf{h} together with some zeros. To explore this relationship, we introduce a shift matrix \mathbf{J} with all 1's in the first sub-diagonal. For convenience, we also use the symbol \mathbf{J}^{-1} to denote \mathbf{J}^T , although \mathbf{J} is singular: $\mathbf{J}^{-1} \triangleq \mathbf{J}^T$, and define \mathbf{J}^0 as an identity matrix. Then, h_i can be obtained by shifting all elements of h_0 up or down by iM positions

$$h_i = \mathbf{J}^{iM} h_0 = \mathbf{J}^{iM} \mathbf{A}\mathbf{h}. \quad (10)$$

To use the subspace technique, we first obtain data covariance matrix based on (4)

$$\mathbf{R} = E \{ \mathbf{y}_{nP} \mathbf{y}_{nP}^H \} = \mathcal{G} \mathbf{E} \{ \mathbf{b}_{nP} \mathbf{b}_{nP}^H \} \mathcal{G}^H + \sigma_v^2 \mathbf{I}. \quad (11)$$

Using (4) and (6), and under the random assumption on both base station's long codes and users' independent inputs of equal power σ_w^2 , one can verify that $\mathbf{E} \{ \mathbf{b}_{nP} \mathbf{b}_{nP}^H \} = \rho \mathbf{I}$, where $\rho = J\sigma_c^2\sigma_w^2$, σ_c^2 is the covariance of $c_{j,n}(k)$. Notice that the orthogonality of users' Hadamard codes has not been invoked at this stage. Then, (11) becomes

$$\mathbf{R} = \rho \mathcal{G} \mathcal{G}^H + \sigma_v^2 \mathbf{I}. \quad (12)$$

Obviously, the columns of \mathcal{G} span the signal subspace of \mathbf{R} . If we define \mathbf{U}_n as the subspace orthogonal to the signal subspace and term it as noise subspace in this paper for convenience, then $\mathbf{U}_n^H \mathcal{G} = \mathbf{0}$ [47]. Since the i th column of \mathcal{G} is given by (10), an accurate channel vector \mathbf{h} should satisfy $\mathbf{U}_n^H \mathbf{J}^{iM} \mathbf{A}\mathbf{h} = \mathbf{0}$ for $i = -q, \dots, 0, \dots, P-1$. Hence, we propose a channel estimation method by minimizing total projection error $\sum_{i=-q}^{P-1} \|\mathbf{U}_n^H \mathbf{J}^{iM} \mathbf{A}\mathbf{h}\|^2$, where $\|\cdot\|$ refers to 2-norm of a vector [51]. Consequently, channel \mathbf{h} is estimated by

$$\mathbf{h} = \arg \min_{\|\boldsymbol{\alpha}\|=1} \boldsymbol{\alpha}^H \mathbf{X} \boldsymbol{\alpha} \quad (13)$$

where $\mathbf{X} = \sum_{i=-q}^{P-1} \mathbf{A}_i^H \mathbf{U}_n \mathbf{U}_n^H \mathbf{A}_i$, $\mathbf{A}_i \triangleq \mathbf{J}^{iM} \mathbf{A}$.

In order to guarantee a unique solution, some conditions need to be imposed on system parameters. Since \mathcal{G} has dimension $MP \times (P+q)$, according to (12), the noise subspace \mathbf{U}_n of \mathbf{R} has dimension $MP - P - q$. Then, the following should be satisfied to ensure the existence of noise subspace

$$M > \frac{P+q}{P}. \quad (14)$$

If $q < P$, then it suffices to choose $M \geq 2$. As q increases, more subchannels are needed. Moreover, all subchannels are required to share no common zeros to guarantee the identification of \mathcal{G} within a scalar ambiguity [47].

IV. DETECTION OF THE DESIRED USER

In this section, we focus on our desired user—user 1 and typical linear detectors to detect its input $w_1(n)$ after channel \mathbf{h} has been estimated based on previously discussed subspace method.

A. Zero Forcing Detection

As we stated before, when we take $M > 1$, the model (4) virtually represents an SIMO system. Therefore, a ZF equalizer can be constructed to extract the sum signal [30], [31]

$$\mathbf{f}_{zf} = \mathcal{G}(\mathcal{G}^H \mathcal{G})^{-1} \mathbf{e} \quad (15)$$

where \mathbf{e} is a unitary vector with its $(q+1)$ th element as 1. Applying the equalizer to \mathbf{y}_{nP} will extract the $(q+1)$ th element of the sum signal \mathbf{b}_{nP} . If we apply the equalizer to P consecutive chip-shifted data vectors $\mathbf{Y}(n) = [\mathbf{y}_{nP}, \dots, \mathbf{y}_{nP+P-1}]$, where $\mathbf{y}_{nP+i} = \mathcal{G}\mathbf{b}_{nP+i} + \mathbf{v}_{nP+i}$, $i = 0, \dots, P-1$

$$\mathbf{b}_{nP+i} = \begin{bmatrix} \mathbf{b}_{nP}^T(i : P+q-1), & \mathbf{b}_{(n+1)P}^T(0 : i-1) \end{bmatrix}^T \quad (16)$$

and $\mathbf{v}_{nP+i} = [\mathbf{v}_{nP}^T(i : P-1), \mathbf{v}_{(n+1)P}^T(0 : i-1)]^T$, we obtain a sequence of sum signals $\sum_j w_j(n) \mathbf{c}_{j,n}^T$. Since $\mathbf{c}_{i,n}^T \mathbf{c}_{j,n}^* = 0$ for $i \neq j$ due to common long codes and orthogonality of Hadamard codes, the desired user's signal $w_1(n)$ is then extracted by despreading the equalized data using the desired user's code vector $\mathbf{c}_{1,n}$

$$\hat{w}_{1,zf}(n) = \mathbf{f}_{zf}^H \mathbf{Y}(n) \mathbf{c}_{1,n}^*. \quad (17)$$

B. MMSE Detection

The ZF equalizer might enhance the effect of noise, especially when the noise is large. A linear MMSE equalizer is expected to outperform the ZF equalizer in that situation. Construction of an MMSE receiver is similar to that of the ZF receiver, i.e., we first construct an MMSE equalizer and apply it to $\mathbf{Y}(n)$ to extract a sequence of sum signals $\sum_j w_j(n) \mathbf{c}_{j,n}^T$ corrupted by residual interference and noise. Then, we pass the equalized data to code decorrelator. The MMSE equalizer might work on partial data vectors for fast convergence under small sample size N , as shown in our simulation section. Suppose the length of the MMSE equalizer is taken as νM , $\nu \leq P$. If the correlation matrix estimated from data vectors of length νM is denoted as

$$\mathbf{R}_\nu = E \{ \mathbf{y}_{nP}(1 : \nu M) \mathbf{y}_{nP}(1 : \nu M)^H \} \quad (18)$$

then the MMSE equalizer obeys the following form [7], [30]:

$$\mathbf{f}_{\text{mmse}} = \mathbf{R}_\nu^{-1} \mathbf{\Gamma}_\nu \mathbf{A} \mathbf{h} \quad (19)$$

where $\mathbf{\Gamma}_\nu = [\mathbf{I}_{\nu M}, \mathbf{0}_{\nu M \times (P-\nu)M}]$ is a selection matrix. To guarantee that $\mathbf{\Gamma}_\nu \mathbf{A} \mathbf{h}$ contains full \mathbf{h} for signal detection, ν should satisfy $\nu \geq q + 1$. Applying the MMSE equalizer to P consecutive partial data vector $\mathbf{Y}_\nu(n) = \mathbf{\Gamma}_\nu \mathbf{Y}(n)$ and decorrelating the equalized data with the desired user's code $\mathbf{c}_{1,n}$ results in the following symbol estimation of $w_1(n)$:

$$\hat{w}_{1,\text{mmse}}(n) = \mathbf{f}_{\text{mmse}}^H \mathbf{Y}_\nu(n) \mathbf{c}_{1,n}^*. \quad (20)$$

C. RAKE Detection

If we partition \mathcal{G} as $\mathcal{G} = [(\mathcal{G}_1)_{PM \times q}, (\mathcal{G}_2)_{PM \times P}]$, then current inputs can be clearly separated from previous inputs on the right-hand side of (4)

$$\begin{aligned} \mathbf{y}_{nP} &= \mathcal{G}_2 \mathbf{c}_{1,n} w_1(n) + \sum_{j=2}^J \mathcal{G}_2 \mathbf{c}_{j,n} w_j(n) \\ &\quad + \sum_{j=1}^J \mathcal{G}_1 \bar{\mathbf{c}}_{j,n-1} w_j(n-1) + \mathbf{v}_{nP}. \end{aligned} \quad (21)$$

It can be found that signature of the desired symbol $w_1(n)$ at time n is $\mathcal{G}_2 \mathbf{c}_{1,n}$. Then, the symbol-level RAKE receiver is constructed as [30], [31]

$$\mathbf{f}_{\text{rake}}(n) = \mathcal{G}_2 \mathbf{c}_{1,n}. \quad (22)$$

At time n , the desired user's symbol is estimated as

$$\hat{w}_{1,\text{rake}}(n) = \mathbf{f}_{\text{rake}}^H(n) \mathbf{y}_{nP}. \quad (23)$$

These linear receivers are coupled with our channel estimator. Their performance should be jointly analyzed with the channel estimator as well.

V. PERFORMANCE ANALYSIS

As observed from (13), (15), (19), and (22), both channel estimator and receivers implicitly depend on \mathbf{R} . They will be perturbed if \mathbf{R} is estimated from N vectors as $\tilde{\mathbf{R}} = (1/N) \sum_{n=1}^N \mathbf{y}_{nP} \mathbf{y}_{nP}^H$. In this section, we will study the statistical performance of the channel estimator in terms of channel MSE and the performance of the receivers in terms of output SINR and BER. Under a large sample size assumption, we apply the perturbation technique [46], [50] to jointly analyze the channel estimator and the receivers. Although up to second-order perturbation results are derived in [50], only first-order perturbation is considered in our analysis. Before we proceed, let us first clarify some notations used in the following analysis: The perturbation is denoted by preceding the corresponding quantity by δ and the perturbed quantity with $\tilde{\cdot}$. For example, $\delta \mathbf{h} = \tilde{\mathbf{h}} - \mathbf{h}$, $\delta \mathbf{R} = \tilde{\mathbf{R}} - \mathbf{R}$. Assume N is sufficiently large such that perturbation technique is applicable.

A. Channel MSE

Since \mathbf{R} is perturbed by $\delta \mathbf{R}$, the first-order perturbation of noise subspace \mathbf{U}_n can be found from [50] to be

$$\delta \mathbf{U}_n \approx -\frac{1}{\rho} (\mathcal{G} \mathcal{G}^H)^\dagger \delta \mathbf{R} \mathbf{U}_n$$

which results in a perturbation to \mathbf{X}

$$\delta \mathbf{X} \approx \sum_{i=-q}^P \mathbf{A}_i^H (\mathbf{U}_n \delta \mathbf{U}_n^H + \delta \mathbf{U}_n \mathbf{U}_n^H) \mathbf{A}_i. \quad (24)$$

Due to $\delta \mathbf{X}$, \mathbf{h} obtained from (13) is perturbed with perturbation $\delta \mathbf{h}$ [50]

$$\delta \mathbf{h} \approx -\mathbf{X}^\dagger \delta \mathbf{X} \mathbf{h} \quad (25)$$

where \dagger represents pseudo-inverse. After substituting (24) in (25), applying $\delta \mathbf{U}_n$, and noticing that $\mathbf{U}_n^H \mathbf{A}_i \mathbf{h} = \mathbf{0}$, we obtain the perturbation of channel estimate

$$\delta \mathbf{h} \approx \frac{1}{\rho} \sum_{i=-q}^{P-1} \mathbf{T}_i \mathbf{U}_n^H \delta \mathbf{R} \mathbf{t}_i \quad (26)$$

where \mathbf{T}_i and \mathbf{t}_i are deterministic quantities

$$\mathbf{T}_i = \mathbf{X}^\dagger \mathbf{A}_i^H \mathbf{U}_n, \quad \mathbf{t}_i = (\mathcal{G} \mathcal{G}^H)^\dagger \mathbf{A}_i \mathbf{h}.$$

Therefore, the covariance of $\delta \mathbf{h}$ becomes

$$\text{Cov}_h \approx \frac{1}{\rho^2} \sum_{i,j} \mathbf{T}_i \mathbf{U}_n^H E \{ \delta \mathbf{R} \mathbf{t}_i \mathbf{t}_j^H \delta \mathbf{R} \} \mathbf{U}_n \mathbf{T}_j^H. \quad (27)$$

Clearly, the covariance depends on the term $E \{ \delta \mathbf{R} \mathbf{t}_i \mathbf{t}_j^H \delta \mathbf{R} \}$. Hence, it suffices to determine a general-form matrix, which is also required later

$$\mathbf{\Psi} = E \{ \delta \mathbf{R} \mathbf{D} \delta \mathbf{R} \} \quad (28)$$

where \mathbf{D} can be replaced by corresponding deterministic quantities respectively later. It is shown in [46] that if all quantities are real, then

$$\mathbf{\Psi} = \frac{\kappa_{4b}}{N} \mathcal{G} [\mathbf{I} \odot (\mathcal{G}^T \mathbf{D} \mathcal{G})] \mathcal{G}^T + \frac{1}{N} \text{tr}(\mathbf{R} \mathbf{D}) \mathbf{R} + \frac{1}{N} \mathbf{R} \mathbf{D}^T \mathbf{R} \quad (29)$$

where \odot represents element-wise multiplication, and κ_{4b} is the fourth-order cumulant of each entry in the sum signal \mathbf{b}_{nP} . For a complex system

$$\mathbf{\Psi} = \frac{\kappa_{4b}}{N} \mathcal{G} [\mathbf{I} \odot (\mathcal{G}^H \mathbf{D} \mathcal{G})] \mathcal{G}^H + \frac{1}{N} \text{tr}(\mathbf{R} \mathbf{D}) \mathbf{R}. \quad (30)$$

Therefore, for a given data model, statistical properties of the inputs and additive noise $\mathbf{\Psi}$ can always be evaluated. Replacing $E \{ \delta \mathbf{R} \mathbf{D} \delta \mathbf{R} \}$ in (27) with (29) or (30), setting $\mathbf{D} = \mathbf{t}_i \mathbf{t}_j^H$, and applying $\mathbf{U}_n^H \mathcal{G} = \mathbf{0}$, one can verify that in either case, (27) becomes $1/(N\rho^2) \sum_{i,j} \mathbf{T}_i \mathbf{U}_n^H \text{tr}(\mathbf{R} \mathbf{t}_i \mathbf{t}_j^H) \mathbf{R} \mathbf{U}_n \mathbf{T}_j^H$. Noticing $\text{tr}(\mathbf{R} \mathbf{t}_i \mathbf{t}_j^H) = \mathbf{t}_j^H \mathbf{R} \mathbf{t}_i$ and $\mathbf{U}_n^H \mathbf{R} \mathbf{U}_n = \sigma_v^2 \mathbf{I}$, (27) further reduces to

$$\text{Cov}_h \approx \frac{\sigma_v^2}{N\rho^2} \sum_{i,j} (\mathbf{t}_j^H \mathbf{R} \mathbf{t}_i) \mathbf{T}_i \mathbf{T}_j^H \quad (31)$$

and the channel MSE is equal to the trace of Cov_h . It is interesting to note that MSE is inversely proportional to ρ^2 , which is $J^2 \sigma_c^4 \sigma_w^4$. As a result, better performance of channel estimation can be expected with more users and higher transmission

power. This appealing property can also be explained from (4), where the sum signal \mathbf{b}_{nP} from J users is transmitted through a common channel at a power J times of the desired user's signal power. Consequently, for fixed transmission power of each user, the more the number of users in the system, the better channel estimation performance.

B. SINRs

SINR is an important performance indicator for receivers. Although ideal SINRs of different receivers can be obtained under perfect conditions, perturbation in channel estimation induced by finite data samples inevitably causes SINRs of those receivers deviated from their optimal values. We will derive perturbed SINRs for the receivers constructed from estimated channel parameters. Moreover, analytical results obtained in this subsection can be further used to predict the BER performance of those receivers, as shown in Section V-C1. For shorter notations, all receiver subscripts are dropped later.

1) *SINR of the ZF Receiver:* According to (17), a ZF equalizer filters the data vector $\mathbf{Y}(n)\mathbf{c}_{1,n}^*$. In order to evaluate SINR, it is essential to express the data vector explicitly in terms of desired symbol, interfering symbols, and noise. If we define $\mathbf{B}_n = [\mathbf{b}_{nP}, \dots, \mathbf{b}_{nP+P-1}]$ and $\mathbf{V}_n = [\mathbf{v}_{nP}, \dots, \mathbf{v}_{nP+P-1}]$, then it is shown in Appendix A that

$$\mathbf{Y}(n)\mathbf{c}_{1,n}^* = \mathcal{G}\mathbf{s}_1(n)w_1(n) + \mathcal{G}\mathbf{H}_{int}(n)\mathbf{w}_{int}(n) + \mathbf{V}(n)\mathbf{c}_{1,n}^* \quad (32)$$

and

$$E\{\mathbf{s}_1(n)\mathbf{s}_1^H(n)\} = \sigma_c^4 \text{diag}\{(P-q) : (P-1) \\ P^2, (P-1) : 1\} \quad (33)$$

$$E\{\mathbf{H}_{int}(n)\mathbf{H}_{int}^H(n)\} = (J-1)\sigma_c^4 \\ \times \text{diag}\{\underbrace{P, \dots, P}_q, 0, \underbrace{P, \dots, P}_{P-1}\} \\ + \sigma_c^4 \text{diag}\{q : 1, 0 : P-1\} \quad (34)$$

$$E\{\mathbf{V}_n\mathbf{c}_{1,n}^*\mathbf{c}_{1,n}^T\mathbf{V}_n^H\} = \gamma\mathbf{I}, \quad \gamma = P\sigma_c^2\sigma_v^2. \quad (35)$$

Based on the above results and the fact that equalizer \mathbf{f} is applied to data vector $\mathbf{Y}(n)\mathbf{c}_{1,n}^*$, the receiver's SINR can be defined as

$$\text{SINR} = \frac{\mathbf{f}^H \mathbf{R}_1 \mathbf{f}}{\mathbf{f}^H \mathbf{R}_{int} \mathbf{f}} \quad (36)$$

where

$$\mathbf{R}_1 = \sigma_w^2 \mathcal{G} E\{\mathbf{s}_1(n)\mathbf{s}_1^H(n)\} \mathcal{G}^H \quad (37)$$

$$\mathbf{R}_{int} = \mathbf{\Sigma} + \gamma\mathbf{I} \\ \mathbf{\Sigma} = \sigma_w^2 \mathcal{G} E\{\mathbf{H}_{int}(n)\mathbf{H}_{int}^H(n)\} \mathcal{G}^H. \quad (38)$$

Obviously, the perturbation of \mathbf{R} will cause the perturbation of the equalizer and, finally, the receiver's SINR perturbed to be

$$\widetilde{\text{SINR}} \approx \frac{\mathbf{f}^H \mathbf{R}_1 \mathbf{f} + E\{\delta \mathbf{f}^H \mathbf{R}_1 \delta \mathbf{f}\}}{\mathbf{f}^H \mathbf{R}_{int} \mathbf{f} + E\{\delta \mathbf{f}^H \mathbf{R}_{int} \delta \mathbf{f}\}}. \quad (39)$$

To evaluate (39), we first obtain $\delta \mathbf{f}$. By (15) and noticing that the perturbed term $(\tilde{\mathcal{G}}^H \tilde{\mathcal{G}})^{-1}$ can be approximated as $(\mathcal{G}^H \mathcal{G})^{-1} -$

$(\mathcal{G}^H \mathcal{G})^{-1} \mathcal{G}^H \delta \mathcal{G} (\mathcal{G}^H \mathcal{G})^{-1} - (\mathcal{G}^H \mathcal{G})^{-1} \delta \mathcal{G}^H \mathcal{G} (\mathcal{G}^H \mathcal{G})^{-1}$ after applying Taylor expansion and keeping only first-order terms, the perturbation of the ZF equalizer is then derived as

$$\delta \mathbf{f} \approx \mathbf{\Pi}^\perp \delta \mathcal{G} (\mathcal{G}^H \mathcal{G})^{-1} \mathbf{e} - (\mathcal{G}^\dagger)^H \delta \mathcal{G}^H (\mathcal{G}^\dagger)^H \mathbf{e} \quad (40)$$

where $\mathbf{\Pi}^\perp \triangleq \mathbf{I} - \mathcal{G} \mathcal{G}^\dagger$, $\mathcal{G}^\dagger \triangleq (\mathcal{G}^H \mathcal{G})^{-1} \mathcal{G}^H$. Based on (40), the terms necessary for computing $\widetilde{\text{SINR}}$ are shown in Appendix B to be

$$E\{\delta \mathbf{f}^H \mathbf{R}_1 \delta \mathbf{f}\} \approx \mathbf{e}^H \mathcal{G}^\dagger E\{\delta \mathcal{G} \mathcal{G}^\dagger \mathbf{R}_1 (\mathcal{G}^\dagger)^H \delta \mathcal{G}^H\} \\ \times (\mathcal{G}^\dagger)^H \mathbf{e} \quad (41)$$

$$E\{\delta \mathbf{f}^H \mathbf{R}_{int} \delta \mathbf{f}\} \approx \mathbf{e}^H \mathcal{G}^\dagger E\{\delta \mathcal{G} \mathcal{G}^\dagger \mathbf{\Sigma} (\mathcal{G}^\dagger)^H \delta \mathcal{G}^H\} \\ \times (\mathcal{G}^\dagger)^H \mathbf{e} \\ + \gamma \mathbf{e}^H \mathcal{G}^\dagger E\{\delta \mathcal{G} (\mathcal{G}^H \mathcal{G})^{-1} \delta \mathcal{G}^H\} \\ \times (\mathcal{G}^\dagger)^H \mathbf{e} \\ + \gamma \mathbf{e}^H (\mathcal{G}^H \mathcal{G})^{-1} E\{\delta \mathcal{G}^H \mathbf{\Pi}^\perp \delta \mathcal{G}\} \\ \times (\mathcal{G}^H \mathcal{G})^{-1} \mathbf{e}. \quad (42)$$

Detailed procedures to simplify the right-hand-side of each equation are also provided in that Appendix.

2) *SINR of the MMSE Receiver:* According to (20), the MMSE equalizer filters the data vector $\mathbf{Y}_\nu(n)\mathbf{c}_{1,n}^*$. Since $\mathbf{Y}_\nu(n) = \mathbf{\Gamma}_\nu \mathbf{Y}(n)$, (37)–(39) can be directly applied after replacing \mathbf{R}_1 with $\mathbf{\Gamma}_\nu \mathbf{R}_1 \mathbf{\Gamma}_\nu^H$ and \mathbf{R}_{int} with $\mathbf{\Gamma}_\nu \mathbf{R}_{int} \mathbf{\Gamma}_\nu^H$. To compute (39), we first obtain the perturbation of the MMSE equalizer. According to (19), noticing that $\tilde{\mathbf{R}}_\nu = \mathbf{R}_\nu + \delta \mathbf{R}_\nu$ and keeping only the first-order terms, $\delta \mathbf{f}$ is found to be

$$\delta \mathbf{f} \approx \mathbf{R}_\nu^{-1} \mathbf{\Gamma}_\nu \mathbf{A} \delta \mathbf{h} - \mathbf{R}_\nu^{-1} \delta \mathbf{R}_\nu \mathbf{R}_\nu^{-1} \mathbf{\Gamma}_\nu \mathbf{A} \mathbf{h}. \quad (43)$$

Noticing that $\mathbf{y}_{nP}(1 : \nu M) = \mathbf{\Gamma}_\nu \mathbf{y}_{nP}$, by (18), it follows that $\mathbf{R}_\nu = \mathbf{\Gamma}_\nu \mathbf{R} \mathbf{\Gamma}_\nu^H$. Its perturbation is then related to $\delta \mathbf{R}$ by $\delta \mathbf{R}_\nu = \mathbf{\Gamma}_\nu \delta \mathbf{R} \mathbf{\Gamma}_\nu^H$. Using this result and substituting (26), $\delta \mathbf{f}$ is related to $\delta \mathbf{R}$ by

$$\delta \mathbf{f} \approx \frac{1}{\rho} \sum_{i=-q}^{P-1} \mathbf{Q}_i \delta \mathbf{R} \mathbf{t}_i - \mathbf{R}_\nu^{-1} \mathbf{\Gamma}_\nu \delta \mathbf{R} \mathbf{\Gamma}_\nu^H \mathbf{f} \quad (44)$$

where $\mathbf{Q}_i = \mathbf{R}_\nu^{-1} \mathbf{\Gamma}_\nu \mathbf{A} \mathbf{T}_i \mathbf{U}_n^H$. Two perturbation quantities in evaluating $\widetilde{\text{SINR}}$ in (39) follow the same form $E\{\delta \mathbf{f}^H \mathbf{\Phi} \delta \mathbf{f}\}$ with corresponding substitution of a deterministic matrix $\mathbf{\Phi}$. Using (44), we have

$$E\{\delta \mathbf{f}^H \mathbf{\Phi} \delta \mathbf{f}\} \approx \frac{1}{\rho^2} \sum_{i,j} \mathbf{t}_i^H E\{\delta \mathbf{R} \mathbf{Q}_i^H \mathbf{\Phi} \mathbf{Q}_j \delta \mathbf{R}\} \mathbf{t}_j \\ + \mathbf{f}^H \mathbf{\Gamma}_\nu E\{\delta \mathbf{R} \mathbf{\Gamma}_\nu^H \mathbf{R}_\nu^{-1} \mathbf{\Phi} \mathbf{R}_\nu^{-1} \mathbf{\Gamma}_\nu \delta \mathbf{R}\} \mathbf{\Gamma}_\nu^H \mathbf{f} \\ - \frac{1}{\rho} \sum_i \mathbf{t}_i^H E\{\delta \mathbf{R} \mathbf{Q}_i^H \mathbf{\Phi} \mathbf{R}_\nu^{-1} \mathbf{\Gamma}_\nu \delta \mathbf{R}\} \mathbf{\Gamma}_\nu^H \mathbf{f} \\ - \frac{1}{\rho} \mathbf{f}^H \mathbf{\Gamma}_\nu \sum_i E\{\delta \mathbf{R} \mathbf{\Gamma}_\nu^H \mathbf{R}_\nu^{-1} \mathbf{\Phi} \mathbf{Q}_i \delta \mathbf{R}\} \mathbf{t}_i. \quad (45)$$

Evaluation of each term on the right-hand side requires a typical matrix $E\{\delta \mathbf{R} \mathbf{D} \delta \mathbf{R}\}$, which can be obtained according to (28) or (29). Finally, SINR directly follows from (39) and (45).

3) *SINR of the RAKE Receiver*: To derive SINR for the RAKE receiver, we start from (21), where \mathbf{y}_{nP} shows clear contributions from the desired symbol, interfering symbols, and noise. Therefore, the output SINR of the rake receiver is computed as

$$\text{SINR} = \frac{\sigma_w^2 E \{ |\mathbf{f}(n)^H \mathcal{G}_2 \mathbf{c}_{1,n}|^2 \}}{\sigma_w^2 E \{ \|\mathbf{f}(n)^H \mathbf{Z}_{int}(n)\|^2 \} + \sigma_v^2 E \{ \|\mathbf{f}(n)\|^2 \}} \quad (46)$$

where $\mathbf{Z}_{int}(n)$ contains all interfering signatures

$$\mathbf{Z}_{int}(n) = [\mathcal{G}_2 \mathbf{c}_{2,n}, \dots, \mathcal{G}_2 \mathbf{c}_{J,n}, \mathcal{G}_1 \bar{\mathbf{c}}_{1,n-1}, \dots, \mathcal{G}_1 \bar{\mathbf{c}}_{J,n-1}]. \quad (47)$$

Since the perturbation of \mathbf{R} causes the perturbation of \mathcal{G} and then the receiver, which finally makes SINR perturbed to be (48), shown at the bottom of the page. To evaluate (48), the perturbation of the RAKE receiver is needed, which by (22) is

$$\delta \mathbf{f}(n) = \delta \mathcal{G}_2 \mathbf{c}_{1,n} \quad (49)$$

where $\delta \mathcal{G}_2$ is obtained from (68)

$$\delta \mathcal{G}_2 = [\mathbf{A}_0 \delta \mathbf{h}, \dots, \mathbf{A}_{P-1} \delta \mathbf{h}]. \quad (50)$$

As shown in Appendix C, those terms required for evaluating (48) can be simplified as

$$\begin{aligned} & E \{ |\mathbf{f}(n)^H \mathcal{G}_2 \mathbf{c}_{1,n}|^2 \} \\ &= \text{vec}^H (\mathcal{G}_2^H \mathcal{G}_2) \\ & \quad \times E \{ (\mathbf{c}_{1,n}^* \otimes \mathbf{c}_{1,n}) (\mathbf{c}_{1,n}^T \otimes \mathbf{c}_{1,n}^H) \} \text{vec} (\mathcal{G}_2^H \mathcal{G}_2) \end{aligned} \quad (51)$$

$$\begin{aligned} & E \{ |\delta \mathbf{f}(n)^H \mathcal{G}_2 \mathbf{c}_{1,n}|^2 \} \\ &= \text{tr} \{ E \{ (\mathbf{c}_{1,n}^* \otimes \mathbf{c}_{1,n}) (\mathbf{c}_{1,n}^T \otimes \mathbf{c}_{1,n}^H) \} \\ & \quad \times (\mathbf{I} \otimes \mathcal{G}_2^H) \mathbf{\Lambda} \text{Cov}_h \mathbf{\Lambda}^H (\mathbf{I} \otimes \mathcal{G}_2^H) \} \end{aligned} \quad (52)$$

$$\begin{aligned} & E \{ \|\mathbf{f}(n)^H \mathbf{Z}_{int}(n)\|^2 \} \\ &= \sum_{j=2}^J \text{vec}^H (\mathcal{G}_2^H \mathcal{G}_2) \frac{E \{ (\mathbf{c}_{1,n}^* \otimes \mathbf{c}_{j,n}) (\mathbf{c}_{1,n}^T \otimes \mathbf{c}_{j,n}^H) \}}{j} \\ & \quad \times \text{vec} (\mathcal{G}_2^H \mathcal{G}_2) + J \sigma_c^4 \text{tr} (\mathcal{G}_2^H \mathcal{G}_1 \mathcal{G}_1^H \mathcal{G}_2) \end{aligned} \quad (53)$$

$$\begin{aligned} & E \{ \|\delta \mathbf{f}(n)^H \mathbf{Z}_{int}(n)\|^2 \} \\ &= \sum_{j=2}^J \text{tr} \{ E \{ (\mathbf{c}_{1,n}^* \otimes \mathbf{c}_{j,n}) (\mathbf{c}_{1,n}^T \otimes \mathbf{c}_{j,n}^H) \} \\ & \quad \times (\mathbf{I} \otimes \mathcal{G}_2^H) \mathbf{\Lambda} \text{Cov}_h \mathbf{\Lambda}^H (\mathbf{I} \otimes \mathcal{G}_2^H) \} \\ & \quad + J \sigma_c^4 \text{tr} \{ E \{ \delta \mathcal{G}_2^H \mathcal{G}_1 \mathcal{G}_1^H \delta \mathcal{G}_2 \} \} \end{aligned} \quad (54)$$

$$E \{ \|\mathbf{f}(n)\|^2 \} = \sigma_c^2 \text{tr} \{ \mathcal{G}_2^H \mathcal{G}_2 \} \quad (55)$$

$$E \{ \|\delta \mathbf{f}(n)\|^2 \} = \sigma_c^2 \text{tr} \left\{ E \left\{ \delta \mathcal{G}_2^H \delta \mathcal{G}_2 \right\} \right\} \quad (56)$$

where $\mathbf{\Lambda}$ is defined as

$$\mathbf{\Lambda} = [\mathbf{A}_0^T, \dots, \mathbf{A}_{P-1}^T]^T \quad (57)$$

and all expected values (underlined) can be finally evaluated, as explained in the Appendix.

C. BER Performance

For each receiver, once its output SINR is evaluated, BER can now be obtained by assuming that the interference is Gaussian distributed. This may not be necessarily correct, but this approximation has been shown to be relatively good [31], [48], especially when a number of interfering users is large. The BER for BPSK information symbol is

$$\text{BER} = Q \left(\sqrt{\text{SINR}} \right) \quad (58)$$

where $Q(x) = 1/\sqrt{2\pi} \int_x^\infty e^{-t^2/2} dt$.

VI. SIMULATION EXAMPLES

In this section, we show the performance of the proposed channel estimator, receivers, and also verify our analytical results by simulations. Comparisons of the proposed approaches with a relevant method in [43] are also included. In implementing [43], two different grouping methods are adopted. We term it as WF1 if the first group contains maximum number of users allowed, as WF2 if the first group only includes the desired user.

In our experiment setup, we consider a DS-CDMA system. The transmitted sequences are drawn from a binary constellation $[-1, 1]$. Each user's short codes are Hadamard codes, which are then multiplied by base station's binary random codes. All users share the same multipath channel, whose coefficients are uniformly distributed in $[-0.5, 0.5]$. We set $P = 16$, $q = 3$ and $M = 2$. User 1 is assumed to be the desired user. All simulation results are the average over 100 Monte Carlo runs. In each realization, the base station codes and multipath channel are randomly generated.

A. Comparison With Analytical Results

In our first group of simulation examples, we compare experimental channel MSEs, output SINRs and BERs with their analytical results respectively. The number of active users in the system is assumed to be 10 for all simulations in this subsection.

Fig. 1 shows MSEs when different data length $N = 100, 500, 1000, 5000, 10000$ are used for channel estimation. The environmental noise is assumed to be white with SNR of 15 dB. The solid line represents experimental result and the dotted line for analytical one computed from the trace of (31) under different N . As expected, the MSE monotonically decreases as N increases. At $N = 500$, MSE shows a satisfactory level of 10^{-3} , while at $N = 10000$, MSE reaches as low as 10^{-5} . Moreover, asymptotic convergence of the experimental MSEs to their analytical values is obvious, indicating that the trace of (31) is a good MSE estimate especially for large N .

$$\widetilde{\text{SINR}} = \frac{\sigma_w^2 E \{ |\mathbf{f}(n)^H \mathcal{G}_2 \mathbf{c}_{1,n}|^2 \} + \sigma_w^2 E \{ |\delta \mathbf{f}(n)^H \mathcal{G}_2 \mathbf{c}_{1,n}|^2 \}}{\sigma_w^2 E \{ \|\mathbf{f}(n)^H \mathbf{Z}_{int}(n)\|^2 \} + \sigma_v^2 E \{ \|\mathbf{f}(n)\|^2 \} + \sigma_w^2 E \{ \|\delta \mathbf{f}(n)^H \mathbf{Z}_{int}(n)\|^2 \} + \sigma_v^2 E \{ \|\delta \mathbf{f}(n)\|^2 \}}. \quad (48)$$

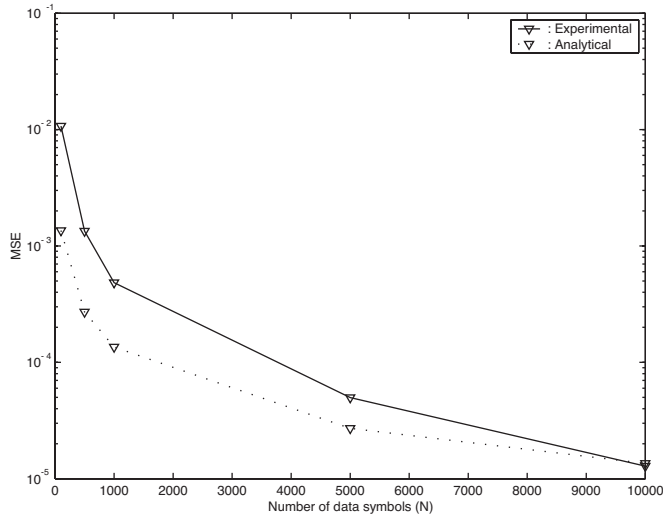
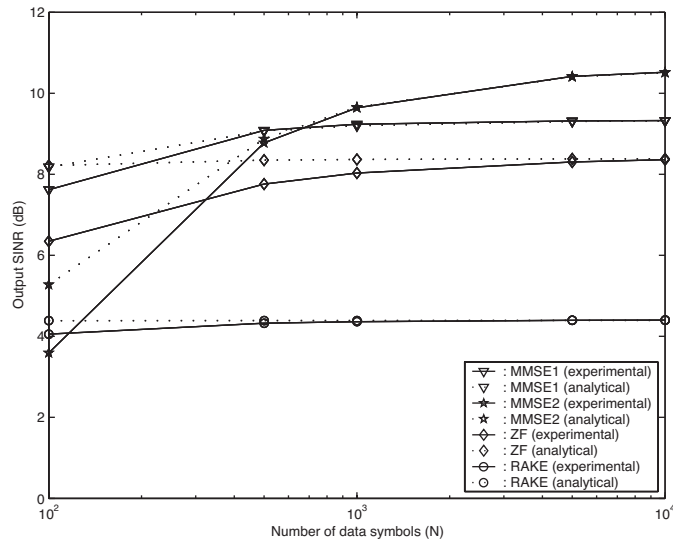
Fig. 1. Channel MSE versus N .Fig. 2. Output SINR versus N .

Fig. 2 illustrates the output SINRs of the ZF, MMSE, and RAKE receivers versus N . The SNR is also set to be 15 dB. The MMSE receivers with $\nu = (q + 1)$ and $\nu = P$ are both implemented and named as MMSE1 and MMSE2, respectively. The experimental results are plotted in solid lines, and the analytical results are plotted in dotted lines. It is observed that each receiver's experimental SINRs approach their corresponding analytical results as N increases, verifying our SINR analysis. On the other hand, it is interesting to note that MMSE2 shows worse performance than MMSE1 when N is small, whereas the former gradually outperforms the latter when N becomes large. The cross point is around $N = 700$. This observation gives us a guideline of choosing the MMSE receiver's length. We thus set $\nu = q + 1$ in all later experiments.

Finally, we compare the experimental BERs with analytical results. In this experiment, we first use a data record of length $N = 500$ for channel estimation and obtain different receivers. Experimental BER is then computed over an independent data of length 5000. The average BERs are plotted and compared

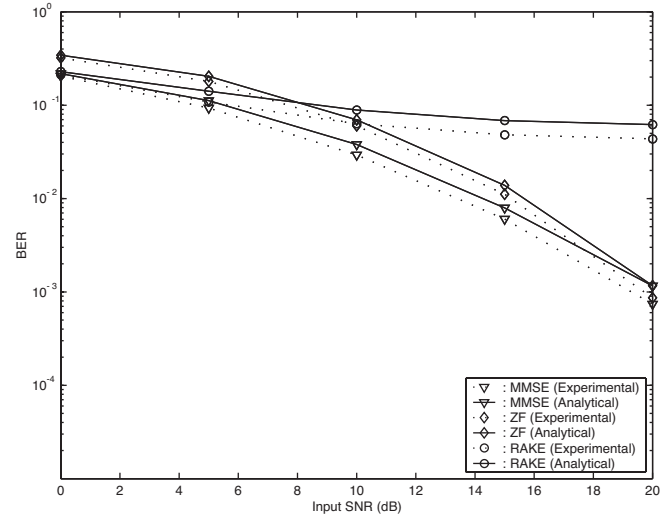


Fig. 3. BER versus SNR.

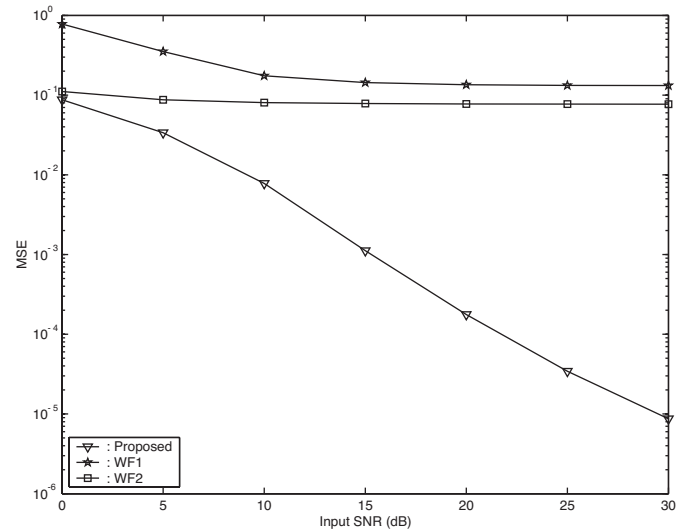


Fig. 4. Channel MSE versus input SNR.

with their analytical ones in Fig. 3. We can see that the experimental results are very close to their analytical ones, especially at low SNRs. The slight differences at high SNRs are caused by the tenuous assumption of Gaussian distribution of interference [31].

B. Comparison With Other Approaches

In this subsection, we compare the performance of the proposed channel estimator receivers with the counterparts of WF1 and WF2. Various situations involving different input signal to noise ratios (SNRs) and variable number of active users are considered in the set of simulation examples.

• Case 1) $J = 10$, different SNRs.

Fig. 4 illustrates the channel estimate MSEs over SNRs of 0 to 30 dB at a step of 5 dB. The proposed channel estimation method significantly outperforms other methods at each SNR examined. Moreover, MSE of the proposed channel estimate almost linearly decreases as SNR increases. By contrast, both WF1 and WF2 demonstrate flat levels though SNR increases.

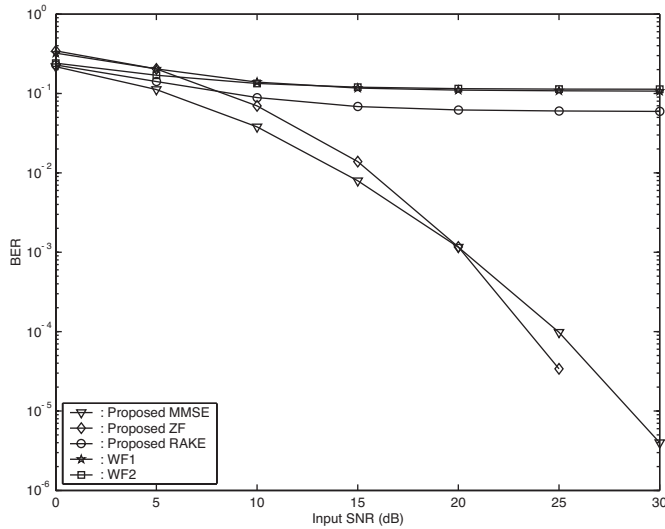


Fig. 5. BER versus input SNR.

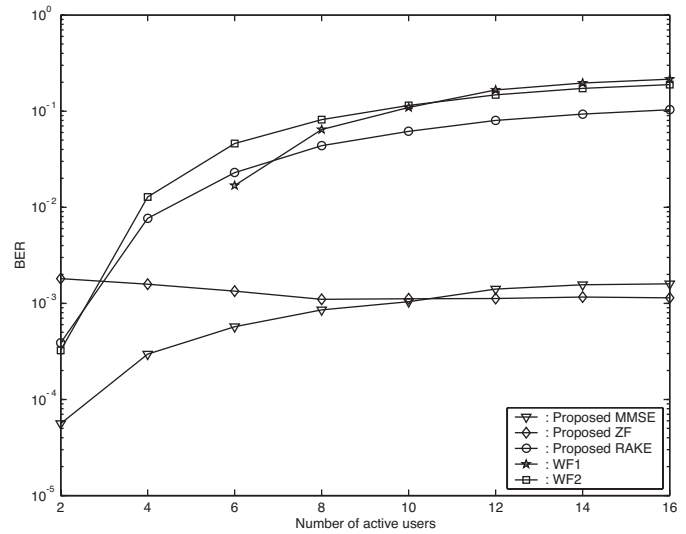


Fig. 7. BER versus number of active users.

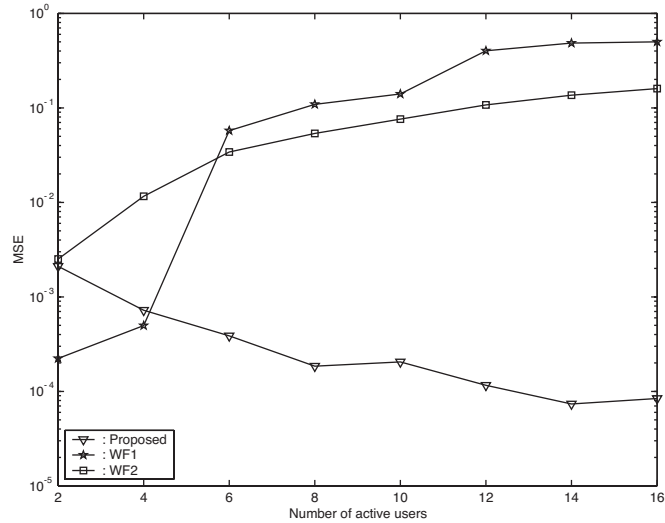


Fig. 6. Channel MSE versus number of active users.

Fig. 5 further plots BER for each receiver in the same situation. At very low SNR, all methods have similar BERs. From moderate to high SNRs, the proposed MMSE and ZF receivers show much lower BERs than WF1 and WF2 due to better channel estimate. The proposed ZF receiver even outperforms the MMSE receiver at high SNRs, where interference is a major concern. Due to the multipath distortion in CDMA downlink, the RAKE receiver does not work satisfactorily. Its BERs stay at a flat level of 0.1. Similarly, both WF1 and WF2 do not perform well either because of large interference from other users.

• Case 2) SNR= 20 dB, variable J .

The MSE and BER performance of each method is examined in different loading situations, where the number of active users varies from 2 to 16 at a step of 2. MSE is plotted in Fig. 6. First, as pointed out after (31), the proposed method shows better performance as number of active users increases in the system, while adversely, WF1 and WF2 show worse per-

formance as system load increases. On the other hand, when system load is very light, i.e., two users, WF1 shows best performance at the cost of using all users' codes. By contrast, WF2, which uses only the desired user's codes, shows the worst performance even when the load is very light. From four users up, the proposed approach starts to significantly outperform other ones. This figure indicates that the proposed channel estimation method can work satisfactorily, irrespective of system load.

The BERs are plotted in Fig. 7. Similar conclusion can be drawn to BER performance. First, we observe that the proposed MMSE and ZF receivers can work satisfactorily over all loading situations. In the case of very light loading, i.e., two to four users, WF1 has lowest BERs by utilizing all users' codes. The proposed MMSE and ZF receivers also have very low BERs over that range. When number of users in the system is more than 4, the performance of WF1 deteriorates substantially. The proposed MMSE receiver, though tending to have slowly increasing BER, still yields an acceptable performance with BER of 10^{-3} in the worst case of full loading. The performance of the ZF receiver is almost unaffected by the loading, due to its desirable characteristics of completely suppressing all interference. On the other hand, the proposed RAKE receiver and WF2 both have worst performance over all loading situations.

VII. CONCLUSION

In this paper, we have proposed a subspace-based channel estimation approach for downlink CDMA system with long codes when spatial/temporal diversity is employed at the receiver. Then, three typical linear receivers (ZF, MMSE, and RAKE) are designed to detect the desired signal. Since the data covariance matrix is used but estimated from finite data samples, perturbation theory is employed to analyze the system performance in terms of channel MSE, output SINR, and BER. Extensive simulation examples justify our analysis. Comparisons with other approaches have also been conducted, which show the superiority of the proposed channel estimator as well as MMSE and ZF receivers.

APPENDIX A
DECOMPOSITION OF $\mathbf{Y}(n)\mathbf{c}_{1,n}^*$ AND DERIVATION
OF SOME STATISTICS

First, we have

$$\mathbf{Y}(n)\mathbf{c}_{1,n}^* = \mathcal{G}\mathbf{B}_n\mathbf{c}_{1,n}^* + \mathbf{V}_n\mathbf{c}_{1,n}^*. \quad (59)$$

After substituting $\mathbf{b}_{nP}, \dots, \mathbf{b}_{nP+P-1}$ with (4), (6) and (16), we have

$$\begin{aligned} \mathbf{B}_n\mathbf{c}_{1,n}^* &= \mathbf{s}_1(n)w_1(n) + \sum_{j=2}^J \mathbf{s}_j(n)w_j(n) \\ &+ \sum_{j=1}^J [\mathbf{s}_j^-(n)w_j(n-1) + \mathbf{s}_j^+(n)w_j(n+1)] \end{aligned} \quad (60)$$

where the desired signature is (61), shown at the bottom of the page, and the interference signature are (62) and (63), also shown at the bottom of the page, and

$$\mathbf{s}_j^+(n) = \begin{bmatrix} \mathbf{0}_{(q+1) \times 1} \\ c_{j,n+1}(0)c_{1,n}^*(P-1) \\ c_{j,n+1}(0)c_{1,n}^*(P-2) + c_{j,n+1}(1)c_{1,n}^*(P-1) \\ \vdots \\ c_{j,n+1}(0)c_{1,n}^*(1) + \dots + c_{j,n+1}(P-2)c_{1,n}^*(P-1) \end{bmatrix}. \quad (64)$$

If we collect all interfering symbols into a big vector $\mathbf{w}_{int}(n)$ and their corresponding signatures into a matrix $\mathbf{H}_{int}(n)$, (32) follows. Next, we derive desired statistics. Let us examine $\mathbf{s}_1(n)$

first. Each $c_{1,n}(k)$ is a product of base station's long code and its Hadamard code. One can observe that except for the $(q+1)$ th row, all other rows involve cross-correlation of codes. Applying the random property of the base station's codes, (33) follows. Since $\mathbf{H}_{int}(n)$ includes $\mathbf{s}_j(n)$, $\mathbf{s}_j^-(n)$ and $\mathbf{s}_j^+(n)$ for symbols at time n , $n-1$, and $n+1$, its statistics can be considered by finding those of $\mathbf{s}_j(n)$, $\mathbf{s}_j^-(n)$ and $\mathbf{s}_j^+(n)$. Following similar steps in obtaining (33) and noticing that the $(q+1)$ th row of $\mathbf{s}_j(n)$ for $j > 1$ is zeroed out due to orthogonality of Hadamard codes, one can verify that

$$\begin{aligned} E \{ \mathbf{s}_j(n)\mathbf{s}_j^H(n) \} &= \sigma_c^4 \text{diag} \{ (P-q) : (P-1), 0, (P-1) : 1 \} \end{aligned} \quad (65)$$

$$\begin{aligned} E \{ \mathbf{s}_j^-(n)(\mathbf{s}_j^-(n))^H \} &= \sigma_c^4 \text{diag} \{ q, \dots, 2, 1, 0, \dots, 0 \} \end{aligned} \quad (66)$$

$$\begin{aligned} E \{ \mathbf{s}_j^+(n)(\mathbf{s}_j^+(n))^H \} &= \sigma_c^4 \text{diag} \{ 0, \dots, 0, 1, 2, \dots, P-1 \} \end{aligned} \quad (67)$$

where “:” represents succession of integers. Since

$$\begin{aligned} E \{ \mathbf{H}_{int}(n)\mathbf{H}_{int}^H(n) \} &= \sum_{j=2}^J E \{ \mathbf{s}_j(n)\mathbf{s}_j^H(n) \} \\ &+ \sum_{j=1}^J E \{ \mathbf{s}_j^-(n)(\mathbf{s}_j^-(n))^H + \mathbf{s}_j^+(n)(\mathbf{s}_j^+(n))^H \} \end{aligned}$$

applying (65)–(67) yields (34). Finally, since \mathbf{V}_n is independent of $\mathbf{c}_{1,n}$, (35) immediately follows.

$$\mathbf{s}_1(n) = \begin{bmatrix} c_{1,n}(0)c_{1,n}^*(q) + \dots + c_{1,n}(P-q-1)c_{1,n}^*(P-1) \\ c_{1,n}(0)c_{1,n}^*(q-1) + \dots + c_{1,n}(P-q)c_{1,n}^*(P-1) \\ \vdots \\ c_{1,n}(0)c_{1,n}^*(0) + \dots + c_{1,n}(P-1)c_{1,n}^*(P-1) \\ c_{1,n}(1)c_{1,n}^*(0) + \dots + c_{1,n}(P-1)c_{1,n}^*(P-2) \\ \vdots \\ c_{1,n}(P-1)c_{1,n}^*(0) \end{bmatrix} \quad (61)$$

$$\mathbf{s}_j(n) = \begin{bmatrix} c_{j,n}(0)c_{1,n}^*(q) + \dots + c_{j,n}(P-q-1)c_{1,n}^*(P-1) \\ c_{j,n}(0)c_{1,n}^*(q-1) + \dots + c_{j,n}(P-q)c_{1,n}^*(P-1) \\ \vdots \\ c_{j,n}(0)c_{1,n}^*(0) + \dots + c_{j,n}(P-1)c_{1,n}^*(P-1) \\ c_{j,n}(1)c_{1,n}^*(0) + \dots + c_{j,n}(P-1)c_{1,n}^*(P-2) \\ \vdots \\ c_{j,n}(P-1)c_{1,n}^*(0) \end{bmatrix} \quad (62)$$

$$\mathbf{s}_j^-(n) = \begin{bmatrix} c_{j,n-1}(P-q)c_{1,n}^*(0) + \dots + c_{j,n-1}(P-1)c_{1,n}^*(q-1) \\ c_{j,n-1}(P-q+1)c_{1,n}^*(0) + \dots + c_{j,n-1}(P-1)c_{1,n}^*(q-2) \\ \vdots \\ c_{j,n-1}(P-1)c_{1,n}^*(0) \\ \mathbf{0}_{P \times 1} \end{bmatrix} \quad (63)$$

APPENDIX B
DERIVATION OF SINR OF THE ZF RECEIVER

Because $\mathbf{\Pi}^\perp \mathcal{G} = \mathbf{0}$ and \mathbf{R}_1 in (37) has a particular structure, (41) readily follows. To obtain this quantity, it suffices to evaluate a typical form $E\{\delta\mathcal{G}\Phi_1\delta\mathcal{G}^H\}$ and then replace Φ_1 by $\mathcal{G}^\dagger \mathbf{R}_1 (\mathcal{G}^\dagger)^H$. Notice that the definition of \mathcal{G} , $\delta\mathcal{G}$ is related to $\delta\mathbf{h}$ as the following:

$$\delta\mathcal{G} = [\mathbf{A}_{-q}\delta\mathbf{h}, \dots, \mathbf{A}_{P-1}\delta\mathbf{h}]. \quad (68)$$

Then

$$E\{\delta\mathcal{G}\Phi_1\delta\mathcal{G}^H\} = \sum_{i,j=1}^{P+q} \Phi_1^{(i,j)} \mathbf{A}_{i-1-q} \text{Cov}_h \mathbf{A}_{j-1-q}^H \quad (69)$$

where $\Phi_1^{(i,j)}$ is the (i,j) th element of Φ_1 , and Cov_h has been derived in (31).

Similarly, since $\mathbf{\Pi}^\perp \Sigma = \mathbf{0}$ and $\mathbf{R}_{int} = \Sigma + \gamma\mathbf{I}$, (42) can be immediately verified. The first and second terms of (42) can be derived by following (69). To obtain the third term, we need $E\{\delta\mathcal{G}^H \mathbf{\Pi}^\perp \delta\mathcal{G}\}$. Considering that the i th column of $\delta\mathcal{G}$ is $\mathbf{A}_{i-1-q}\delta\mathbf{h}$, the (i,j) th element of this matrix is $E\{\delta\mathbf{h}^H \Theta_{i,j} \delta\mathbf{h}\}$, where $\Theta_{i,j} = \mathbf{A}_{i-1-q}^H \mathbf{\Pi}^\perp \mathbf{A}_{j-1-q}$. Substituting (26) for $\delta\mathbf{h}$, we have

$$E\{\delta\mathbf{h}^H \Theta_{i,j} \delta\mathbf{h}\} \approx \frac{1}{\rho^2} \sum_{k_1, k_2=-q}^{P-1} \mathbf{t}_{k_1}^H \times E\{\delta\mathbf{R} \mathbf{U}_n \mathbf{T}_{k_1}^H \Theta_{i,j} \mathbf{T}_{k_2} \mathbf{U}_n^H \delta\mathbf{R}\} \mathbf{t}_{k_2}. \quad (70)$$

The expectation on the right-hand side is readily obtained according to (28) and (29). Therefore, SINR follows.

APPENDIX C
DERIVATION SINR OF THE RAKE RECEIVER

A. Desired Symbol's Power and Its Perturbation

First, using trace and vec operations [51], the power of the desired symbol is derived as

$$\begin{aligned} E\{|\mathbf{f}(n)^H \mathcal{G}_2 \mathbf{c}_{1,n}|^2\} &= E\{\text{tr}\{\mathcal{G}_2^H \mathcal{G}_2 \mathbf{c}_{1,n} \mathbf{c}_{1,n}^H \\ &\quad \times \mathcal{G}_2^H \mathcal{G}_2 \mathbf{c}_{1,n} \mathbf{c}_{1,n}^H\}\} \\ &= E\{\text{vec}^H(\mathcal{G}_2^H \mathcal{G}_2) \text{vec}(\mathbf{c}_{1,n} \mathbf{c}_{1,n}^H) \\ &\quad \times \mathcal{G}_2^H \mathcal{G}_2 \mathbf{c}_{1,n} \mathbf{c}_{1,n}^H\} \\ &= \text{vec}^H(\mathcal{G}_2^H \mathcal{G}_2) \\ &\quad \times E\{(\mathbf{c}_{1,n}^* \otimes \mathbf{c}_{1,n}) \\ &\quad \times (\mathbf{c}_{1,n}^T \otimes \mathbf{c}_{1,n}^H)\} \text{vec}(\mathcal{G}_2^H \mathcal{G}_2). \end{aligned} \quad (71)$$

Since $\mathbf{c}_{1,n}$ is a random vector, the expectation term can be directly obtained as [49] for real codes

$$E\{(\mathbf{c}_{1,n}^* \otimes \mathbf{c}_{1,n}) (\mathbf{c}_{1,n}^T \otimes \mathbf{c}_{1,n}^H)\} = \kappa_{4c} \mathbf{X}_1 + \sigma_c^4 \mathbf{X}_2 + \sigma_c^4 \text{vec}(\mathbf{I}) \text{vec}(\mathbf{I})^H + \sigma_c^4 \mathbf{I} \quad (72)$$

and for complex codes

$$E\{(\mathbf{c}_{1,n}^* \otimes \mathbf{c}_{1,n}) (\mathbf{c}_{1,n}^T \otimes \mathbf{c}_{1,n}^H)\} = \kappa_{4c} \mathbf{X}_1 + \sigma_c^4 \text{vec}(\mathbf{I}) \text{vec}(\mathbf{I})^H + \sigma_c^4 \mathbf{I} \quad (73)$$

where κ_{4c} is the fourth-order cumulant of the spreading codes

$$\begin{aligned} \mathbf{X}_1 &= \text{diag}\{\mathbf{a}_1 \mathbf{a}_1^T, \dots, \mathbf{a}_P \mathbf{a}_P^T\} \\ \mathbf{a}_i &= \underbrace{[0, \dots, 0]_{i-1}}_{i-1}, \underbrace{[1, 0, \dots, 0]_{P-i}}_{P-i}^T \end{aligned}$$

and \mathbf{X}_2 is partitioned into $P \times P$ sub-blocks with the (i,j) th sub-block $\mathbf{a}_j^T \mathbf{a}_i$. Following similar steps, replacing $\mathcal{G}_2^H \delta\mathcal{G}_2$ by $\mathcal{G}_2^H \delta\mathcal{G}_2 \mathbf{I}$, and using vec operations, the perturbation of the power of the desired symbol is derived as

$$\begin{aligned} E\{|\delta\mathbf{f}(n)^H \mathcal{G}_2 \mathbf{c}_{1,n}|^2\} &= E\{\text{vec}^H(\mathcal{G}_2^H \delta\mathcal{G}_2) (\mathbf{c}_{1,n}^* \otimes \mathbf{c}_{1,n}) \\ &\quad \times (\mathbf{c}_{1,n}^T \otimes \mathbf{c}_{1,n}^H) \\ &\quad \times \text{vec}(\mathcal{G}_2^H \delta\mathcal{G}_2)\} \\ &= \text{tr}\{E\{(\mathbf{c}_{1,n}^* \otimes \mathbf{c}_{1,n}) \\ &\quad \times (\mathbf{c}_{1,n}^T \otimes \mathbf{c}_{1,n}^H)\} \\ &\quad \times E\{\text{vec}(\mathcal{G}_2^H \delta\mathcal{G}_2) \\ &\quad \times \text{vec}^H(\mathcal{G}_2^H \delta\mathcal{G}_2)\}\} \\ &= \text{tr}\{E\{(\mathbf{c}_{1,n}^* \otimes \mathbf{c}_{1,n}) (\mathbf{c}_{1,n}^T \otimes \mathbf{c}_{1,n}^H)\} \\ &\quad \times (\mathbf{I} \otimes \mathcal{G}_2^H) \\ &\quad \times E\{\text{vec}(\delta\mathcal{G}_2) \text{vec}(\delta\mathcal{G}_2)^H\} \\ &\quad \times (\mathbf{I} \otimes \mathcal{G}_2^H)\} \end{aligned} \quad (74)$$

where the second equality invokes a mild assumption on the independence of $\mathbf{c}_{1,n}$ and $\delta\mathcal{G}_2$. Although this assumption is inaccurate for moderate N , it yields satisfactory prediction of receiver's performance for large N , as verified by simulations. Noticing (57), the expectation term $E\{\text{vec}(\delta\mathcal{G}_2) \text{vec}(\delta\mathcal{G}_2)^H\}$ is then obtained as

$$E\{\text{vec}(\delta\mathcal{G}_2) \text{vec}(\delta\mathcal{G}_2)^H\} = \mathbf{\Lambda} \text{Cov}_h \mathbf{\Lambda}^H. \quad (75)$$

Combining (74) and (75), the perturbed desired power in (52) follows.

B. Interfering Symbols' Power and Its Perturbation

According to (47) and following similar steps in (71), the interfering symbols' power is given by

$$\begin{aligned} E\{|\mathbf{f}(n)^H \mathbf{Z}_{int}(n)|^2\} &= \sum_{j=2}^J E\{|\mathbf{f}(n)^H \mathcal{G}_2 \mathbf{c}_{j,n}|^2\} \\ &\quad + \sum_{j=1}^J E\{|\mathbf{f}(n)^H \mathcal{G}_1 \bar{\mathbf{c}}_{j,n-1}|^2\} \\ &= \sum_{j=2}^J \text{vec}^H(\mathcal{G}_2^H \mathcal{G}_2) \\ &\quad \times E\{(\mathbf{c}_{1,n}^* \mathbf{c}_{1,n}^T) \otimes (\mathbf{c}_{j,n} \mathbf{c}_{j,n}^H) \\ &\quad \times \text{vec}(\mathcal{G}_2^H \mathcal{G}_2)\} \\ &\quad + \sum_{j=1}^J \text{vec}^H(\mathcal{G}_1^H \mathcal{G}_1) \\ &\quad \times E\{(\mathbf{c}_{1,n}^* \mathbf{c}_{1,n}^T) \\ &\quad \otimes (\bar{\mathbf{c}}_{j,n-1} \bar{\mathbf{c}}_{j,n-1}^H)\} \\ &\quad \times \text{vec}(\mathcal{G}_1^H \mathcal{G}_1) \end{aligned} \quad (76)$$

where $\mathbf{c}_{1,n}$ and $\mathbf{c}_{j,n}$ are dependent with each other since they share the same base station codes. If we denote the j th user's Hadamard codes as β_j , and the base station codes at time instant n as ξ_n , then $\mathbf{c}_{j,n} = \Omega_j \xi_n$, where $\Omega_j = \text{diag}\{\beta_j\}$ is a $P \times P$ diagonal matrix with its (k, k) th element as $\beta_j(k)$. Based on the new notation of $\mathbf{c}_{j,n}$ and using the property of Kronecker product [51], we immediately obtain

$$E \{ (\mathbf{c}_{1,n}^* \mathbf{c}_{1,n}^T) \otimes (\mathbf{c}_{j,n} \mathbf{c}_{j,n}^H) \} = (\Omega_1^* \otimes \Omega_j) \times E \{ (\xi_n^* \otimes \xi_n) (\xi_n^T \otimes \xi_n^H) \} (\Omega_1^T \otimes \Omega_j^H) \quad (77)$$

where $E \{ (\xi_n^* \otimes \xi_n) (\xi_n^T \otimes \xi_n^H) \}$ can be similarly calculated as (72) or (73). On the other hand, $\mathbf{c}_{1,n}$ is independent of $\mathbf{c}_{j,n-1}$ since they correspond to base station's codes at different time instants. Therefore, the second expectation on the right-hand side of (76) is easily computed as

$$E \{ (\mathbf{c}_{1,n}^* \mathbf{c}_{1,n}^T) \otimes (\bar{\mathbf{c}}_{j,n-1} \bar{\mathbf{c}}_{j,n-1}^H) \} = \sigma_c^4 \mathbf{I}. \quad (78)$$

Combining (76)–(78), (53) follows. Now, let us turn to the perturbation of interfering symbols' power, which by definition is

$$E \{ \|\delta \mathbf{f}(n)^H \mathbf{Z}_{int}(n)\|^2 \} = \sum_{j=2}^J E \{ \|\delta \mathbf{f}(n)^H \mathcal{G}_2 \mathbf{c}_{j,n}\|^2 \} + \sum_{j=1}^J E \{ \|\delta \mathbf{f}(n)^H \mathcal{G}_1 \bar{\mathbf{c}}_{j,n-1}\|^2 \}. \quad (79)$$

Taking similar steps as (74) and using (75) and (78), (54) immediately follows, where $E \{ \delta \mathcal{G}_2^H \mathcal{G}_1 \mathcal{G}_1^H \delta \mathcal{G}_2 \}$ has a similar form as $E \{ \delta \mathcal{G}^H \mathbf{\Pi}^\perp \delta \mathcal{G} \}$. Its (i, j) th element can be similarly evaluated as (70) after considering (50)

$$E \{ \delta \mathbf{h}^H \mathbf{\Theta}_{i,j} \delta \mathbf{h} \} \approx \frac{1}{\rho^2} \sum_{k_1, k_2=0}^{P-1} \mathbf{t}_{k_1}^H \times E \{ \delta \mathbf{R} \mathbf{U}_n \mathbf{T}_{k_1}^H \mathbf{\Theta}_{i,j} \mathbf{T}_{k_2} \mathbf{U}_n^H \delta \mathbf{R} \} \mathbf{t}_{k_2} \quad (80)$$

where $\mathbf{\Theta}_{i,j} = \mathbf{A}_{i-1}^H \mathcal{G}_1 \mathcal{G}_1^H \mathbf{A}_{j-1}$.

C. Noise Power and Its Perturbation

Replacing $\mathbf{f}(n)$ by (22) and noticing that $\mathbf{c}_{1,n}$ is independent of noise and $E \{ \mathbf{c}_{1,n} \mathbf{c}_{1,n}^H \} = \sigma_c^2 \mathbf{I}$, noise power and its perturbation are readily derived as (55) and (56), where $E \{ \delta \mathcal{G}_2^H \delta \mathcal{G}_2 \}$ in (56) can be obtained similarly as above.

REFERENCES

- [1] *Physical Layer Standard for CDMA2000 Standards for Spread Spectrum Systems—TIA/EIA/IS-2000.2-A*, TIA/EIA Interim Stand., Mar. 2000.
- [2] (2001) 3GPP TS 25.2-Series (Physical Layer), Technical Specification. Third Generation partnership Project. [Online]. Available: <http://www.3gpp.org>; <http://www.3gpp2.org>; <http://www.itu.int/itmt>
- [3] A. Viterbi, *Principles of Spread Spectrum Communication*. Reading, MA: Addison-Wesley, 1995.
- [4] S. Verdú, *Multuser Detection*. New York: Cambridge Univ. Press, 1998.
- [5] S. Buzzi and H. V. Poor, "Channel estimation and multiuser detection in long-code DS/CDMA systems," *IEEE J. Select. Areas Commun.*, vol. 19, pp. 1476–1487, Aug. 2001.
- [6] A. Klein, G. K. Kaleh, and P. W. Baier, "Zero forcing and minimum mean-square-error equalization for multiuser detection in code-division multiple-access channels," *IEEE Trans. Veh. Technol.*, vol. 45, pp. 276–287, May 1996.
- [7] H. Liu and M. D. Zoltowski, "Blind equalization in antenna array CDMA systems," *IEEE Trans. Signal Processing*, vol. 45, pp. 161–172, Jan. 1997.
- [8] M. D. Zoltowski and J. Ramos, "Blind adaptive beamforming for CDMA based PCS/cellular," in *Proc. Asilomar Conf.*, Nov. 1995.
- [9] Y. Chen, M. D. Zoltowski, J. Ramos, C. Chatterjee, and V. P. Roychowdhury, "Reduced-dimension blind space-time 2-D RAKE receivers for DS-CDMA communication systems," *IEEE Trans. Signal Processing*, vol. 48, pp. 1521–1536, June 2000.
- [10] J. Ramos, M. D. Zoltowski, and H. Liu, "A low-complexity space-time RAKE receiver for DS-CDMA communications," *IEEE Signal Processing Lett.*, vol. 4, pp. 262–265, Sept. 1997.
- [11] —, "Low-complexity space-time processor for DS-CDMA communications," *IEEE Trans. Signal Processing*, vol. 48, pp. 39–52, Jan. 2000.
- [12] K. Li and H. Liu, "Channel estimation for DS-CDMA with aperiodic spreading codes," in *Proc. ICASSP*, vol. 5, 1999, pp. 2535–2538.
- [13] M. Torlak, B. L. Evans, and G. Xu, "Blind estimation of FIR channels in CDMA systems with aperiodic spreading sequences," in *Proc. Asilomar Conf.*, vol. 1, 1997, pp. 495–499.
- [14] S. Bhashyam and B. Aazhang, "Multiuser channel estimation and tracking for long-code CDMA systems," *IEEE Trans. Commun.*, vol. 50, pp. 1081–1090, July 2002.
- [15] C. J. Escudero, U. Mitra, and D. T. M. Slock, "A toeplitz displacement method for blind multipath estimation for long code DS/CDMA signals," *IEEE Trans. Signal Processing*, vol. 49, pp. 654–665, Mar. 2001.
- [16] Z. Xu and M. Tsatsanis, "Blind channel estimation for long code multiuser CDMA systems," *IEEE Trans. Signal Processing*, vol. 48, pp. 988–1001, Apr. 2000.
- [17] Z. Xu, "Low complexity multiuser channel estimation with aperiodic spreading codes," *IEEE Trans. Signal Processing*, vol. 49, pp. 2813–2822, Nov. 2001.
- [18] —, "Computationally efficient multiuser detection for aperiodically spreading CDMA systems," in *Proc. ICASSP*, vol. 4, 2001.
- [19] N. D. Sidiropoulos, G. B. Giannakis, and R. Bro, "Blind PARAFAC receivers for DS-CDMA systems," *IEEE Trans. Signal Processing*, vol. 48, pp. 810–823, Mar. 2000.
- [20] Z. Yang and X. Wang, "Blind turbo multiuser detection for long-code multipath CDMA," *IEEE Trans. Commun.*, vol. 50, pp. 112–125, Jan. 2002.
- [21] P. Schramm and R. R. Muller, "Spectral efficiency of CDMA systems with linear MMSE interference suppression," *IEEE Trans. Commun.*, vol. 47, pp. 722–731, May 1999.
- [22] S. Verdú and S. Shamai, "Spectral efficiency of CDMA with random spreading," *IEEE Trans. Inform. Theory*, vol. 45, pp. 622–640, Mar. 1999.
- [23] U. Madhow and M. L. Honig, "On the average near-far resistance for MMSE detection of direct sequence CDMA signals with random spreading," *IEEE Trans. Inform. Theory*, vol. 45, pp. 2039–2045, Sept. 1999.
- [24] S. Parkvall, "Variability of user performance in cellular DS-CDMA-long versus short spreading sequences," *IEEE Trans. Commun.*, vol. 48, pp. 1178–1187, July 2000.
- [25] K. Tang, P. H. Siegel, and L. B. Milstein, "A comparison of long versus short spreading sequences in coded asynchronous DS-CDMA systems," *IEEE J. Select. Areas Commun.*, vol. 19, pp. 1614–1624, Aug. 2001.
- [26] U. Mitra, "Comparison of maximum-likelihood-based detection for two multirate access schemes for CDMA signals," *IEEE Trans. Commun.*, vol. 47, pp. 64–77, Jan. 1999.
- [27] A. Klein, "Data detection algorithms specially designed for the downlink of CDMA mobile radio systems," in *Proc. Veh. Technol. Conf.*, vol. 1, 1997, pp. 203–207.
- [28] K. Li and H. Liu, "A new blind receiver for downlink DS-CDMA communications," *IEEE Commun. Lett.*, vol. 3, pp. 193–195, July 1999.
- [29] C. D. Frank and E. Visotsky, "Adaptive interference suppression for direct-sequence CDMA systems with long spreading codes," in *Proc. Allerton Conf.*, 1998.
- [30] C. D. Frank, E. Visotsky, and U. Madhow, "Adaptive interference suppression for the downlink of a direct sequence CDMA system with long spreading sequences," *J. VLSI*, vol. 30, no. 1–3, pp. 273–291, Mar. 2002.
- [31] T. P. Krauss, W. J. Hillery, and M. D. Zoltowski, "Downlink specific linear equalization for frequency selective CDMA cellular systems," *J. VLSI*, vol. 30, no. 1–3, pp. 143–161, Jan.–Mar. 2002.
- [32] G. Xu, H. Liu, L. Tong, and T. Kailath, "A least-squares approach to blind channel identification," *IEEE Trans. Signal Processing*, vol. 43, pp. 2982–2993, Dec. 1995.

- [33] T. P. Krauss and M. D. Zoltowski, "Blind channel identification on CDMA forward link based on dual antenna receiver at handset and cross-relation," in *Proc. Asilomar Conf.*, vol. 1, 1999, pp. 75–79.
- [34] S. Chowdhury and M. D. Zoltowski, "Adaptive MMSE equalization for wideband CDMA forward link with time-varying frequency selective channels," in *Proc. ICASSP*, vol. III, 2002, pp. 2609–2612.
- [35] S. Chowdhury, M. D. Zoltowski, and J. C. Goldstein, "Reduced-rank adaptive MMSE equalization for high-speed CDMA forward link with sparse multipath channels," *Proc. Asilomar Conf.*, vol. 2, pp. 965–969, 2000.
- [36] G. E. Bottomley, "Optimizing the RAKE receiver for the CDMA downlink," in *Proc. Veh. Technol. Conf.*, 1993, pp. 742–745.
- [37] G. E. Bottomley, T. Ottosson, and Y. Wang, "A generalized RAKE receiver for interference suppression," *IEEE J. Select. Areas Commun.*, vol. 18, pp. 1536–1545, Aug. 2000.
- [38] M. J. Heikkila, P. Komulainen, and J. Lilleberg, "Interference suppression in CDMA downlink through adaptive channel equalization," in *Proc. Veh. Technol. Conf.*, vol. 2, 1999, pp. 978–982.
- [39] S. Werner and J. Lilleberg, "Downlink channel decorrelation in CDMA systems with long codes," in *Proc. Veh. Technol. Conf.*, vol. 2, 1999, pp. 1614–1617.
- [40] K. Hooli, M. Latva-aho, and M. Juntti, "Multiple access interference suppression with linear chip equalizers in WCDMA downlink receivers," in *Proc. GLOBECOM*, vol. 1a, 1999, pp. 467–471.
- [41] I. Ghauri and D. T. M. Slock, "Blind maximum sinr receiver for the DS-CDMA downlink," in *Proc. ICASSP*, vol. 5, 2000, pp. 2485–2488.
- [42] G. Montalbano, I. Ghauri, and D. T. M. Slock, "Spatio-temporal array processing for aperiodic CDMA downlink transmission," in *Proc. Asilomar Conf.*, vol. 2, 1999, pp. 912–916.
- [43] A. J. Weiss and B. Friedlander, "Channel estimation for DS-CDMA downlink with aperiodic spreading codes," *IEEE Trans. Commun.*, vol. 47, pp. 1561–1569, Oct. 1999.
- [44] Z. Xu and D. Reitz, "Subspace-based channel estimation for CDMA downlink with aperiodic spreading codes and multiple subchannels," in *Proc. Asilomar Conf.*, vol. 2, 2001, pp. 1728–1732.
- [45] Y. Sung and L. Tong, "A projection-based semi-blind channel estimation for long-code WCDMA," in *Proc. ICASSP*, vol. III, 2002, pp. 2245–2248.
- [46] Z. Xu, "On the second-order statistics of the weighted sample covariance matrix," *IEEE Trans. Signal Processing*, vol. 51, pp. 527–534, Feb. 2003.
- [47] E. Moulines, P. Duhamel, J.-F. Cardoso, and S. Mayrargue, "Subspace methods for the blind identification of multichannel FIR filters," *IEEE Trans. Signal Processing*, vol. 43, pp. 516–525, Feb. 1995.
- [48] A. H. Madsen and X. Wang, "Performance of blind and group-blind multiuser detectors," *IEEE Trans. Inform. Theory*, vol. 48, pp. 1849–1872, July 2002.
- [49] Z. Xu, "Asymptotic performance of subspace methods for synchronous multirate CDMA systems," *IEEE Trans. Signal Processing*, vol. 50, pp. 2015–2026, Aug. 2002.
- [50] —, "Perturbation analysis for subspace decomposition with applications in subspace-based algorithms," *IEEE Trans. Signal Processing*, vol. 50, pp. 2820–2830, Nov. 2002.
- [51] P. Lan and M. Tismenetsky, *The Theory of Matrices*, 2 ed. San Diego, CA: Academic, 1985.



Ping Liu (S'00) received the B.S. and M.S. degrees in electronic engineering from Sichuan University, Chendu, China, in 1990 and 1993, respectively, and the M.Eng. degree in electrical and electronic engineering from Nanyang Technological University, Singapore, in 1999. She is currently pursuing the Ph.D. degree in electrical engineering at University of California, Riverside.

From 1993 to 1997, she was a senior software engineer with International Software Development Company, Shenzhen, China. From April 1999 to August 1999, she was a research engineer with Kent Ridge Digital Labs, Singapore. Her research interests are in the area of blind channel estimation and equalization, wireless multiuser communications, and digital signal processing.



Michael D. Zoltowski (F'99) was born in Philadelphia, PA, on August 12, 1960. He received both the B.S. and M.S. degrees in electrical engineering with highest honors from Drexel University, Philadelphia, PA, in 1983 and the Ph.D. degree in systems engineering from the University of Pennsylvania, Philadelphia, in 1986.

From 1982 to 1986, he was an Office of Naval Research Graduate Fellow. In Fall 1986, he joined the faculty of Purdue University, West Lafayette, IN, where he currently holds the position of Professor of electrical and computer engineering.

Dr. Zoltowski was the recipient of the IEEE Outstanding Branch Counselor Award for 1989–1990, the Ruth and Joel Spira Outstanding Teacher Award for 1990–1991, and the 2001–2002 The Wilfred Hesselberth Award for Teaching Excellence. In August 2001, he was named a University Faculty Scholar. He received a 2002 Technical Achievement Award from the IEEE Signal Processing Society. He is also a co-recipient of the IEEE Communications Society 2001 Leonard G. Abraham Prize Paper Award in the Field of Communications Systems. He was recently selected as a 2003 Distinguished Lecturer for the IEEE Signal Processing Society. He received the IEEE Signal Processing Society's 1991 Paper Award (Statistical Signal and Array Processing Area), "The Fred Ellersick MILCOM Award for Best Paper in the Unclassified Technical Program" at the IEEE Military Communications (MILCOM '98) Conference, and a Best Paper Award at the IEEE International Symposium on Spread Spectrum Techniques and Applications (ISSSTA 2000). He has served as an associate editor for both the IEEE TRANSACTIONS ON SIGNAL PROCESSING and the IEEE COMMUNICATIONS LETTERS. Within the IEEE Signal Processing Society, he has been a member of both the Technical Committee for the Statistical Signal and Array Processing Area and the DSP Education Committee. He is currently a member of both the Technical Committee on Signal Processing for Communications (SPC) and the Technical Committee on Sensor and Multichannel (SAM) Processing. In addition, from 1998 to 2001, he was a Member-at-Large of the Board of Governors and Secretary of the IEEE Signal Processing Society.



Zhengyuan Xu (S'97–M'99–SM'02) received both the B.S. and M.S. degrees in electronic engineering from Tsinghua University, Beijing, China, in 1989 and 1991, respectively, and the Ph.D. degree in electrical engineering from Stevens Institute of Technology, Hoboken, NJ, in 1999.

From 1991 to 1996, he worked as an engineer and department manager at the Tsinghua Unisplendour Group Corp., Tsinghua University. Since 1999, he has been with the Department of Electrical Engineering, University of California, Riverside, as

an assistant professor. His current research interests include advanced signal processing, multirate communication, multiuser detection, and *ad hoc* and wireless sensor networking.

Dr. Xu received the Outstanding Student Award and the Motorola Scholarship from Tsinghua University as well as the Peskin Award from Stevens Institute of Technology. He also received the Academic Senate Research Award and the Regents' Faculty Award from University of California, Riverside. He is an associate editor for the IEEE TRANSACTIONS ON VEHICULAR TECHNOLOGY and the IEEE COMMUNICATIONS LETTERS.